

Response to reviewers' comments on "Kinetics, SOA yields and chemical composition of secondary organic aerosol from β -caryophyllene ozonolysis with and without nitrogen oxides between 213 and 313 K" (acp-2021-1067)

The authors kindly thank the reviewers for the careful review of our manuscript, and the quite helpful comments and suggestions. All the comments are addressed below point by point, with our responses in blue, and the corresponding revisions to the manuscript in red. All updates of the original manuscript are marked in the revised version.

Reviewer #1

The authors investigated the SOA formation from the ozonolysis of β -caryophyllene (BCP) at different temperatures in an atmospheric simulation chamber and showed that the SOA particle yields increase with decreasing temperatures. The authors attributed this to the decrease of the vapour pressure of the oxidation products at reduced temperatures and supported this by showing that a larger fraction of products with lower number of oxygen atoms were present at lower temperatures compared to higher, where higher O:C was observed. They also provide, for the first time, reaction rate coefficients for the reaction of BCP with ozone at different temperatures. Furthermore, in each experiment, after the initial amounts of BCP were consumed, additional BCP, ozone and nitrogen dioxide were added to the chamber to form SOA in the presence of nitrate radicals. Advanced mass spectrometry techniques were used to investigate the chemical composition of the gas and particle phase in each experimental setting and showed that the chemical composition had significant temperature dependence.

Overall, I believe that the manuscript falls within the scope of ACP as it provides new information for the SOA formation, composition and kinetics from the oxidation of BCP and importantly, their temperature dependence. I recommend this work for publication after a few major and some minor considerations have been addressed.

General comments:

1. The study suggests that the experiments were conducted under representative of the real atmosphere conditions, which might be true for the selected temperature and relative humidity conditions. However, the study uses unrealistically high oxidant and precursor concentrations that could have altered the fate of the radicals. I am therefore wondering how the resulted chemical regime of the experiments could have affected the results presented and their implications to the real atmosphere.

This is indeed an important question relevant for most simulation chamber studies. The initial mixing ratios of BCP in our experiments ranged between 3 and 12 ppb and are thus about two orders of magnitude higher than those typically observed in forests. In contrast, the initial ozone levels varied between ~25-75 ppb, which are close to its average ambient levels, and were only

increased to about 300 ppb in the later stages of the experiments. The elevated concentration compared to typical ambient levels may typically affect reactions with a non-linear dependence on concentration. These can be for example reactions of two monomers leading to the formation of dimers. However, in our study we observed increasing fractions of dimers formed for lower temperatures and for lower initial BCP concentrations. Hence, if the concentration levels would have affected the dimer formation we would have underestimated the dimer formation compared to the ambient atmosphere.

2. All the experiments aside from the different temperatures were also conducted under substantially different relative humidity (RH) conditions (13-97%). It was recently shown that the BCP-SOA chemical composition could be considerably affected by the RH levels (e.g., Kundu et al., 2017), therefore how the difference in the RH between the experiments conducted in this study could have affected the reported results? I understand that the authors try to capture the variation of the temperature and RH found in the different layers of the atmosphere. However, I believe that the potential implications of the different RH levels should be included in the interpretation of the results.

The relative humidity and temperature have an influence on viscosity of the SOA particles (Li and Shiraiwa, 2019; Maclean et al., 2021) and the temperature obviously influences the reaction pathways leading to different chemical composition. Thus, the relative humidity may potentially affect mainly condensed phase reactions. However, for the gas phase reactions the water concentration is relevant and therefore we tried to keep it close to typical ambient levels or at least sufficiently high. Kundu et al. (2017) did not see substantial differences in the chemical composition as long as the water vapor concentration was not artificially low. For the higher temperatures the relative humidity was lower but this would not reduce the viscosity substantially. For the particles formed at the lower temperatures, the relative humidity was significantly higher to minimize the reduction in particle viscosity due to the lower temperatures. Therefore, we cannot exclude completely that the changing humidity has no influence on our results. Nonetheless, we think that the SOA composition we have observed is dominated by gas phase reactions with sufficient water concentrations compared to ambient conditions and that the potential impact of relative humidity on condensed phase reactions was minimized by increasing relative humidity with decreasing temperature, maybe except for the lowermost temperature (213 K). We have included these aspects in the conclusions section as follows:

“Please note that we cannot exclude completely that the changing humidity in our experiments has no influence on our results. Nonetheless, we think that the SOA composition we have observed is dominated by gas phase reactions with sufficient water concentrations compared to ambient conditions and that the potential impact of relative humidity on condensed phase reactions was minimized by increasing relative humidity with decreasing temperature (Li and Shiraiwa, 2019; Maclean et al., 2021), maybe except for the lowermost temperature (213 K).”

3. The study compares the SOA yields obtained in this study with values obtained previously in the literature and attributes the observed differences to the potentially different oxidative conditions. Whilst this, at least in part might be true, it may be worthwhile considering the potentially different losses and partitioning of the semi-volatile vapours in the different chambers - even so considering the different materials of the chambers (i.e., Teflon vs Aluminum).

Additional discussion should probably be included when interpreting and discussing the SOA yield results.

We calculated wall losses of particles and semi volatile vapours in the AIDA aluminium chamber with the aerosol dynamic model COSIMA (Naumann, 2003; Saathoff et al., 2009) and corrected the yields accordingly. Our yields are 40-55% lower than literature values obtained from studies in Teflon chambers. These studies also applied reasonable wall loss corrections. Typically, the losses of acidic gases are larger in an aluminium chamber compared to a Teflon chamber and it may be the opposite for particle losses. This depends on the age of the chamber walls, potential electrostatic losses, and volume to surface ratio of the chamber, etc. It is therefore not easy to determine the impact of the different wall losses and the wall loss corrections. For our study the wall losses and corresponding corrections were relatively small and can't explain deviations of 40-55%. We can only speculate if too high wall loss corrections for the studies in the Teflon chamber contribute to this difference. We have added the following text to section 3.2 on particle mass yields:

“For our study the wall losses and corresponding corrections were relatively small and can't explain deviations of 40-55%. Typically, the losses of acidic gases are larger in an aluminium chamber compared to a Teflon chamber and it may be the opposite for particle losses. This depends on the age of the chamber walls, potential electrostatic losses, and the volume to surface ratio of the chamber. It is therefore not easy to determine the impact of the different wall losses and the wall loss corrections. We can only speculate if too high wall loss corrections for the studies in the Teflon chamber contribute to the different yields.”

4. In my opinion, a lot more information is required for the operation and data analysis of the FIGARO-CIMS dataset. The authors report a considerably large fraction of products with particularly high molecular weight (>400 Th). It would be helpful for the readers to know the range the mass calibration was conducted, the associated peak assignment errors and thereby, the confidence in the results presented. Furthermore, additional information about the particle-phase background subtraction and sampling strategy would be beneficial.

We included I_3^- ($m/z = 381$ Th) and a dominating product ion $C_{30}H_{48}O_5I^-$ ($m/z = 615$ Th) for the mass calibration. With this procedure we found the mass defect of most compounds in a good linear correlation with m/z , and without ‘bend’ at high masses. We added a plot of mass defects as a function of mass ranging from 46-780 Th in the supplement as figure S3. We constrained the peak assignment errors to 20 ppm.

We took a particle background filter before the start of each experiment, using the same sampling method (flow rate of 6.4 L/min, sampling system, Teflon filter type, and sampling time of 10 minutes) as employed for the particle. Thus, for the dataset presented in this manuscript we collected ten particle background filters in total. Those background filters were then thermally desorbed in FIGAERO-iodide-CIMS in the same way as the particle loaded filter samples. We subtracted the mass spectra of these background filter samples from those of the particle loaded samples from the same experiment. We have added this information to the method section as follows:

“We included I^- ($m/z = 127$ Th), $I(H_2O)^-$ ($m/z = 145$ Th), $I(CH_2O_2)^-$ ($m/z=173$ Th), I_3^- ($m/z = 381$ Th), and a dominating product ion $C_{30}H_{48}O_5I^-$ ($m/z = 615$ Th) for our mass calibration. With this

procedure we found the mass defect of most compounds in a good linear correlation and without significant deviations at high masses (cf. Figure S3). We constrained the peak assignment errors to 20 ppm.”

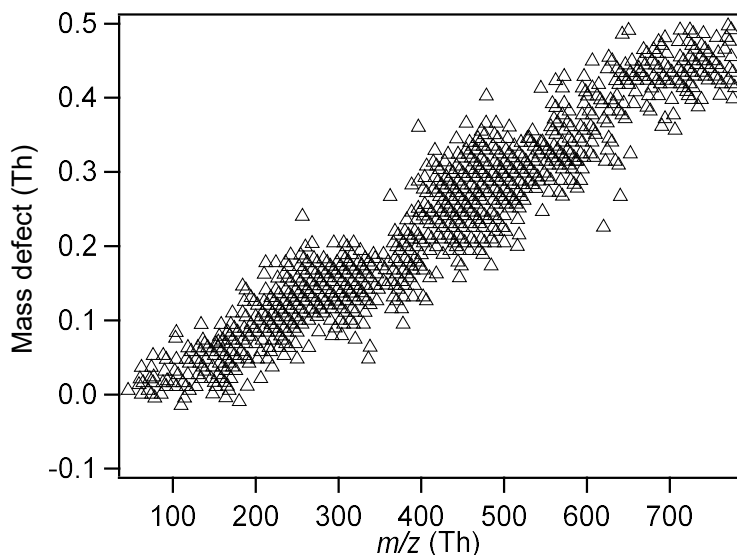


Figure S3. Plot of mass defect corresponding to the mass of molecules assigned for the BCP SOA in this work.

“We subtracted the mass spectra of the background filter samples from those of the particle loaded filter samples for the same experiments.”

5. I believe that the absorptive partitioning should be considered when discussing and interpreting the results and particularly, the different levels of absorptive mass in each experimental setting. For example, higher SOA yields and lower O:C have been observed at the lower temperature experiments opposed to those conducted at higher temperatures (that exhibited lower yield + higher O:C). Could this behaviour be attributed to the higher levels of absorptive mass present at the higher yield experiments, enabling the partitioning of the less oxygenated (and consequently more volatile species) to the condensed phase, thus decreasing the average O:C? To better understand this, I think that it would be beneficial, at least in the supporting information, to show the time-series of the SOA mass in each experimental setting. This effect could be even more pronounced when the authors compare the ozonolysis experiments with those in the presence of NO_3 . The ozonolysis experiments entailed the formation of SOA from the nucleation of the oxidation products, whereas those formed in the presence of NO_3 involve the condensation of the species on the top of those pre-existing particles. Intuitively, the partitioning behaviour of the species in each of these cases could be significantly altered due to the significantly different absorptive mass present and thereby could have affected the reported results and their comparison.

The time series of SOA masses and particle number size distributions for each experiment are shown in figures 2 and S4. Furthermore, the dependence of SOA yields as a function of organic aerosol mass available for partitioning are shown in figure S6. To compare the yields, we present them in figure 4 for the same organic aerosol mass of $10 \mu\text{g m}^{-3}$. It was our aim to have similar aerosol mass loadings for all experiments to ensure the best possible comparability. We managed to have the organic aerosol mass concentrations available for partitioning during the initial ozonolysis steps in the range of $4.5\text{--}31.5 \mu\text{g m}^{-3}$ for the temperatures between 213 and 313 K.

Therefore, we consider the experiments as comparable in terms of a potential influence of absorptive partitioning. This is also the case for reaction steps with NO_3 radicals for which the organic aerosol mass concentrations ranged between 14 and $41 \mu\text{g m}^{-3}$. Since we had relatively similar and sufficient organic aerosol mass levels available for partitioning, the observed differences in chemical composition should be governed by the changing chemistry, mainly in the gas phase. We have added the following text to the method section to illustrate this:

“We tried to have similar organic particle mass concentrations among the different experiments in order to limit a potential influence of absorptive partitioning on the comparison among different temperatures. The organic aerosol mass levels were in the range of $4.5\text{-}31.5 \mu\text{g m}^{-3}$ for the initial ozonolysis and between 14 and $41 \mu\text{g m}^{-3}$ for the reaction step with NO_3 radicals. Since we had relatively similar and sufficient organic aerosol mass levels available for partitioning, the observed differences in chemical composition should be governed by the changing chemistry, mainly in the gas phase.”

6. Further to the above, all the experiments were conducted in the absence of seed particles. Could the potentially different particle number (and thereby surface area) in each experimental setting have affected the partitioning of the species between the particle phase and the chamber walls? What would be the implications on the results? Again, time-series of the particle number/surface area in each experiment might be beneficial.

We didn't have significant differences in wall losses among the different experiment which would affect their comparability. Time series for all experiments are given in figures 2 and S4. The mean geometric diameters of the particles for all experiments are given in Table 1. Due to the low vapor pressures of the majority of the reaction products, the minor influence of wall losses, the rapid nucleation, and the availability of a sufficiently large condensation sink we would expect very similar results in the presence of seed particles.

Specific comments

L57, L87 and L217: As from 2020, IUPAC has released updated values for the reaction rate coefficients for major organic compounds, including BCP that can be found on Cox et al., (2020) and Mellouki et al., (2021). I recommend those values to be used throughout the manuscript, including the calculations performed.

We implemented these values in the manuscript.

L126: “saturated with its vapour” how this was confirmed?

The BCP (liquid at 298K) was added to the chamber with a synthetic air flow of $0.01 \text{ m}^3/\text{min}$ guided through a reservoir filled with liquid BCP. The air flow is potentially saturated with BCP. Since we didn't proof this we changed the sentence in the manuscript as follows:

“BCP (98%, Carl Roth GmbH) was added to the AIDA chamber with a flow of $0.01 \text{ m}^3/\text{min}$ of synthetic air potentially saturated with its vapour at 298K.”

L140: Why the authors decided to get a slower decay only in the 273K experiments and not the rest? How this could have affected the results?

As mentioned in the method section we also performed additional experiments at 243 and 258 K with lower initial ozone concentrations and didn't find significant differences in the mass spectra at similar temperatures (cf. Figure R1), e.g. confirming the general trend observed. Therefore, we conclude that the chemical composition at 273K was not significantly affected by the lower initial ozone level.

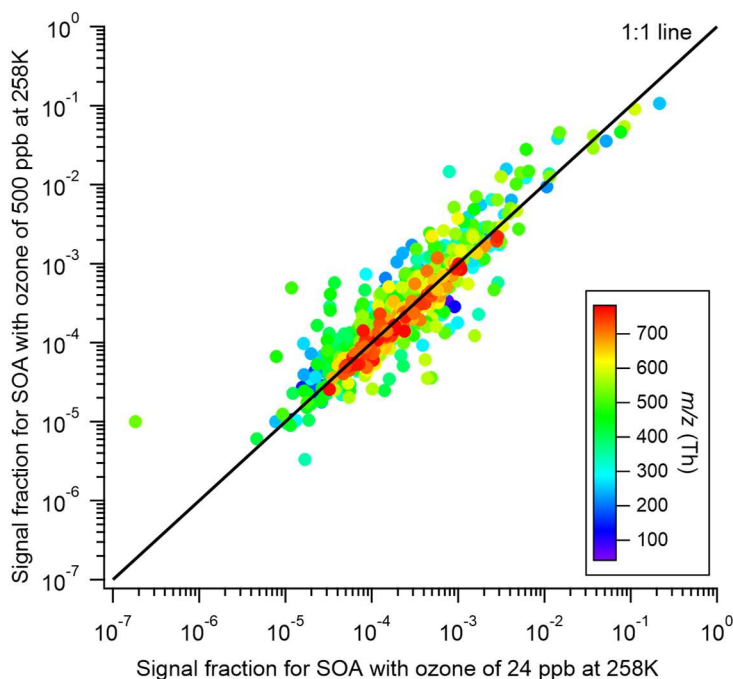


Figure R1. Scatter plot of particle phase signal for individual organic compounds of β -caryophyllene SOA with initial and subsequent ozone concentration of 24 ppb and 258 ppb, respectively.

L171: I think that it would be beneficial for the readers if the authors provide a more detailed description of their error propagation estimates.

We have included this in more detail as follows:

“In this study, we calibrated the mixture of toluene and BCP with a solvent of *n*-hexane using LCU. We obtained a similar sensitivity for toluene using the LCU and a gas cylinder with a toluene standard. Then we calculated the sensitivity of BCP relative to the sensitivity of toluene. This resulted in 36.2 ncps/ppb for the parent ion ($C_{15}H_{25}^+$, m/z 205) of BCP. The total uncertainty of the quantification of BCP was estimated to $\sim 20\%$ by including the uncertainties of toluene in the gas standard ($\sim 10\%$), the LCU calibration procedure ($\sim 15\%$), and the fragmentation pattern of BCP ($\sim 5\%$).”

L183: What was the relative ionisation efficiency of the AMS and how it was obtained?

The ionization efficiency of the AMS we used was $(1.52 \pm 0.1) \times 10^{-7}$, which was obtained according to our calibration using 300 nm ammonium nitrate particles. We generated dry ammonium nitrate particles in 300 nm with a series of concentrations using an atomizer. The particles were then detected by SMPS and AMS separately. Then we fitted the concentration detected by AMS (the sum concentration of m/z 30 and m/z 46) and SMPS (assuming the particles were spherical and the density was 1.72 g cm^{-3}). The slope of the fit line was obtained as the ionization efficiency value. We did the ionization efficiency calibration at the start and the end of the campaign.

L191: where the remaining $0.003 \text{ m}^3/\text{min}$ are going? I presume to the exhaust but it would be nice if this was clarified in the revised manuscript.

Indeed, the $0.003 \text{ m}^3/\text{min}$ went to a bypass flow used to enhance the sample gas flow, and hence reducing the residence time of gaseous compounds in the gas inlet. We clarified this in the manuscript as follows:

“The bypass flow of $0.003 \text{ m}^3/\text{min}$ was used to reduce the residence time in the sampling line.”

L204-207: In line with the general comment #4, it is unclear how the background subtraction was conducted. I think that additional information for the data processing would be beneficial.

We added this information to the method section as follows:

“We subtracted the mass spectra of the background filter samples from those of the particle loaded filter samples for the same experiments.”

L231: It is unclear to me how the COSIMA accounts for the losses of semi-volatile vapours. Furthermore, to what extent the interactions of the aluminium walls of the AIDA with the losses of particles and the partitioning of the semi-volatile vapours were considered? Does this have any implications for the reported results?

The COSIMA model allows to calculate the wall loss of semi volatile gases for which the rate limiting step is their diffusion through the laminar boundary layer at the wall (Saathoff et al., 2009). Furthermore, the model allows to calculate the particle losses, e.g. by sedimentation or diffusion. As stated in the manuscript, these losses were relatively small on the time scale of the experiments, and they were corrected and thus did not affect the results.

L246-250: BCP secondary additions are not visible in Fig.2, while the third is not described in the methods section nor related data are shown in table 1. I think that such information should be detailed in the experimental conditions section.

As ozone was in a relatively large excess before the second BCP injection, BCP reacted too quickly to be detected by PTR-MS. Thus, no significant increase of BCP can be seen in the Fig.2. We added the BCP addition steps in the methods section as follows and show them also in Fig 2 and Fig S4:

“At the initial phase of each experiment, BCP was depleted completely by ozonolysis and SOA was formed. Then a second addition of BCP generated more SOA mass. Due to the large excess of ozone, BCP could not be measured during the subsequent additions. The corresponding conditions are marked as 1a-5a in Table 1. Subsequently, NO₂ (1000 ppm of 99.5% purity in nitrogen 99.999%, Basi Schöberl GmbH) was added to the reaction mixture still containing an excess of ozone. Another step of SOA formation was then initialized by adding more BCP in the presence of NO₃ radicals.”

L259: I generally do not support the calculation of the total mass concentrations from the FIGAERO-CIMS assuming maximum sensitivity for all the compounds detected, given that a lot of work has been devoted to illustrate the issue of the differential sensitivity in the instrument along with potential ways to constrain such issues (e.g., Lopez-Hilfiker et al., 2016). Nonetheless, I do see some value in comparing the estimated trends with those derived from the HR-AMS. I would recommend however, definite quantitative statements such as those presented on that sentence to be soften.

The comparison of the mass concentrations derived from AMS, SMPS, and FIGAERO-CIMS using the maximum sensitivity (22 cps ppt⁻¹) demonstrates that the results from FIGAERO-CIMS reflect only a fraction of the total SOA mass even if assuming an average maximum sensitivity. We modified the sentence as follows:

“The total organic mass concentration detected by FIGAERO-iodide-CIMS, if assuming an average maximum sensitivity for all compounds, corresponds to 36-61 % of the total organic aerosol mass measured by AMS.”

L279: Do you have any evidence that the SOA particle yields from the OH oxidation should be higher than the ozonolysis? For other precursors, such as the α -pinene, the SOA yields from the O₃ oxidations have been found to be higher than the OH-initiated oxidation.

Also for SOA formation from reactions of α -pinene with ozone and OH radicals, higher SOA yields were observed in presence of OH radicals (Donahue et al., 2012). Since we did not use OH radical scavengers we expected higher SOA yields compared to those studies using the scavengers. However, we observed lower yields without OH radical scavengers. Please note that the OH radicals yields from the BCP ozonolysis are relatively small and thus their impact may be limited.

L400: How the contribution of the NO₃ oxidation was estimated at different temperatures, given that there are no available BCP reaction rates with temperature? What would be the error in those estimates? Perhaps additional information about the box modelling should be included in the manuscript.

In estimating the NO₃ concentration, our box model considered the temperature dependent reactions between NO₂, O₃, NO₃, N₂O₅, HNO₃ and corresponding wall losses as outlined in the supplement. However, we did not consider the NO₃ radicals reacting with BCP or its oxidation products. Thus, the modelled NO₃ concentrations should be considered as upper limits. We added this information to the reaction scheme given in the supplements as follows:

“Please note that we did not include the reactions of NO_3 radicals with BCP or its oxidation products in our box model calculations, which was used to estimate the NO_3 radical concentrations. Therefore, these NO_3 radical concentrations must be considered as upper limits.”

And in the manuscripts as:

“Please note that these values should be considered as upper limits due to other potential sinks for NO_3 radicals.”

L411: Why the formation of $\text{C}_{15}\text{H}_{25}\text{O}_7\text{N}$ indicates that BCP is reacting directly with NO_3 and the formation and not that certain pre-existing O_3 -initiated oxidation products are reacting with NO_3 ? Perhaps a more descriptive approach will benefit the readers.

The gas phase signal of $\text{C}_{15}\text{H}_{25}\text{O}_7\text{N}$ I had no significant change after the NO_2 addition, however, it had a steep increase immediately after the 3rd addition of BCP (Figure R2). Thus, we regard $\text{C}_{15}\text{H}_{25}\text{O}_7\text{N}$ as a product from NO_3 reacting with BCP directly but not with the pre-existing O_3 -initiated oxidation products. This has also been clearly stated in the manuscript (line 449-451).

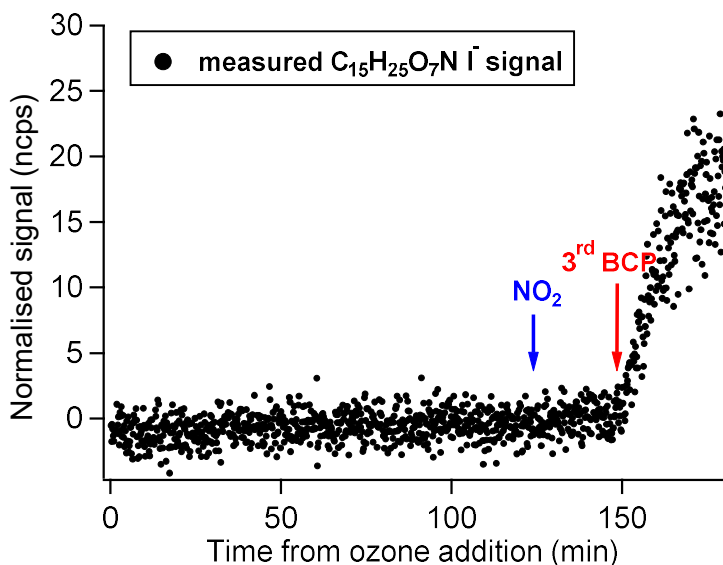


Figure R2. Time evolution of $\text{C}_{15}\text{H}_{25}\text{O}_7\text{N}$ I ion.

L421: How the mass of the organic nitrates was calculated from the HR-AMS measurements? It is known that it is challenging to retrieve N-containing species from that instrument (e.g., Farmer et al., 2010), so it would be helpful if more information was provided.

We determined the mass concentration of the organonitrates (OrgNO_3 , i.e., organonitrates) from AMS data, by assuming an average OrgNO_3 molecular weight of 330 g mol^{-1} based on the most abundant molecules ($\text{C}_{15}\text{H}_{25}\text{O}_7\text{N}$ and $\text{C}_{15}\text{H}_{25}\text{O}_9\text{N}$) detected by FIGAERO-iodide-CIMS. We have added this information to the method section as follows:

“In the absence of inorganic species, we calculated the mass concentration of the organonitrates (OrgNO_3 , i.e., organonitrates) from AMS data, by assuming an average OrgNO_3 molecular weight

of 330 g mol^{-1} based on the most abundant molecules ($\text{C}_{15}\text{H}_{25}\text{O}_7\text{N}$ and $\text{C}_{15}\text{H}_{25}\text{O}_9\text{N}$) detected by FIGAERO-iodide-CIMS.”

L451: Perhaps adding a reference about the potential thermal instability of N-containing compounds at 313K would be beneficial here. If so, how about their decomposition in the FIGAERO-CIMS?

It has been found the thermal decomposition of alkyl nitrates can be negligible with desorption temperature between 60-100 °C, while the peroxy nitrates have substantial thermal loss in the isoprene and monoterpene derived SOA (Francisco and Krylowski, 2005; Lee et al., 2016). In the β -caryophyllene system, we compared the thermal behaviors of the three abundant N-containing ions at 313K in Figure R3 below. The most dominating N-containing compound $\text{C}_{15}\text{H}_{23}\text{O}_9\text{N}_1$ was desorbed mostly between 60-120°C, and hence the contribution of thermal decomposed ions to this molecule could be negligible. However, a lighter N-containing molecule $\text{C}_5\text{H}_7\text{O}_6\text{N}_1$ has an unexpected T_{max} of $\sim 160^\circ\text{C}$, and it was more likely to be a thermally decomposed ion from larger oligomers, e.g. dimeric peroxy nitrates. In addition, the potential contributions from thermal decomposition ($\text{C}_{1-13}\text{H}_y\text{O}_z\text{N}_1$ I⁻ ions) showed a positive temperature dependence (Figure R4), and accounted for 23% of total signals of the N-containing compounds. This may also be an explanation for the weaker increase of their fraction observed for 313K.

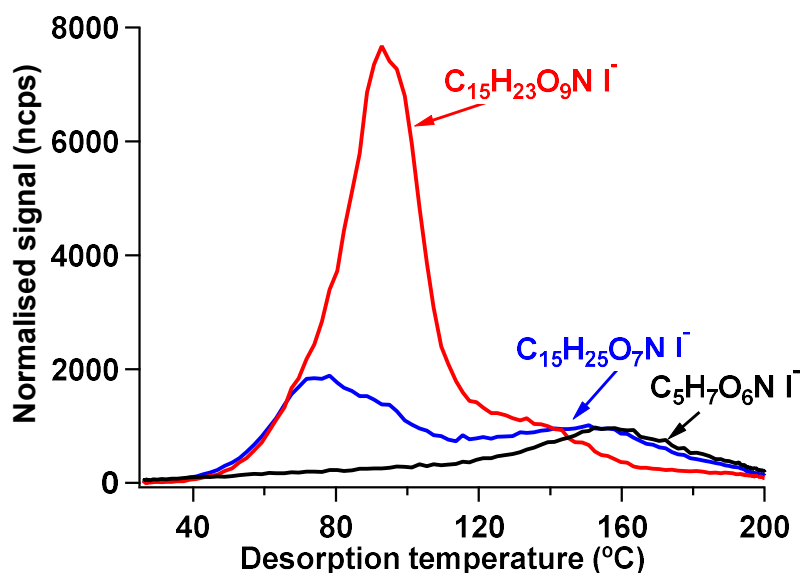


Figure R3. Thermogram of $\text{C}_{15}\text{H}_{23}\text{O}_9\text{N}_1 \text{ I}^-$ ion (red), $\text{C}_{15}\text{H}_{25}\text{O}_7\text{N}_1 \text{ I}^-$ ion (blue) and $\text{C}_5\text{H}_7\text{O}_6\text{N}_1 \text{ I}^-$ (black).

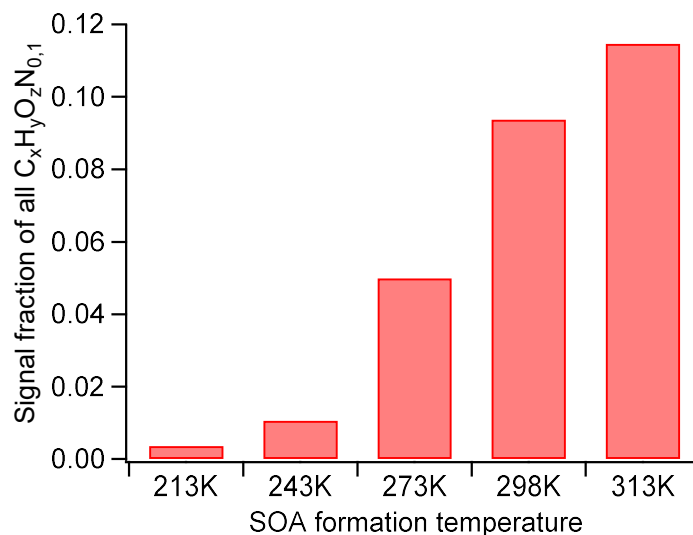


Figure R4. Signal fractions of $C_{1-13}HONI$ ions to the total signals (sum of CHO and CHON molecules) at all SOA formation temperatures.

We added the references about the thermal instability of N-containing compounds to the manuscript as follows:

“On the other hand, thermal instability of some N-containing compounds formed at 313K, e.g. peroxy nitrates (Francisco and Krylowski, 2005; Lee et al., 2016), can also be an explanation for the weaker increase of their fraction observed for 313K. For example, the potential contributions from thermal decomposition ($C_{1-13}H_yO_zN_1$ I- ions) showed a positive temperature dependence. Also, abundant N-containing ions, such as low molecular-weight molecule $C_5H_7O_6N_1$, desorbed substantially between 120-200°C, and had an unexpected high T_{max} of about 160°C.”

Technical corrections

L101: “big condensation potential”, I think that the authors mean that at lower temperatures the vapour pressure of the components is lower and thereby altering the partitioning behaviour of the species. Probably this sentence needs some rephrasing and appropriate references.

We have modified this sentence to:

“In addition, at lower temperatures also semi volatile vapours alter their partitioning behaviour due to reduced vapour pressures.”

L103: this sentence is a bit difficult to understand, please re-write.

We have modified this sentence to:

“Despite of the potentially important role of BCP oxidation products in NPF and their high condensation and SOA formation potential, studies on the temperature dependence of SOA formation from ozonolysis of BCP is still scarce.”

L115: “bottom”, I assume of the chamber. Please re-write.

We have modified this sentence to:

“It is operated as a continuously stirred reactor with mixing times of 1-2 minutes achieved using a fan about 1 m above the bottom of the chamber.”

L168: please remove the parenthesis from the contribution of the major ions

We have given results plus uncertainties consistently with parenthesis like: (29±1)% and believe it is not misleading here.

L381-386: these are not annotated in any of the figures and are a bit difficult to follow, please re-write.

We reformulated this referring to the related figures as follows:

“Two different dimeric patterns appear in the temperature range of 213-313K (Figures 6 and 7). One pattern is represented by molecular formulae of $C_{28-30}H_{42-48}O_{5-8}$ at 213-243K (marked as low temperature group, LT-group), and the other pattern is represented by $C_{28-30}H_{36-44}O_{9-11}$ at 273-313K (marked as high temperature group, HT-group).”

L390: From figure 2 second addition of BCP appears to be between 150-160 min instead of 180-190 min.

We have corrected this.

L430: This sentence is not very clear could you please re-write? Also, could this shift be attributed to the different total absorptive mass present enabling the partitioning of the less oxygenated and consequently more volatile species to the particle phase (see also general comment #5)?

We think the differences observed can't be explained by different total absorptive organic particle masses as they don't differ that much as outlined above. We have tried to formulate the sentence clearer as follows:

“The most abundant mass spectral peak of all organic compounds without nitrogen at 298-313K was not $C_{14}H_{22}O_7$ as for pure ozonolysis, but $C_{15}H_{24}O_4$ in the presence of NO_2 and NO_3 radicals. This is attributed to additional formation of pure MLOCs.”

L435-436 and L439-440: these sentences are a bit difficult to understand, please re-write.

We have modified these sentence as follows:

“However, it cannot be excluded that they could be formed by the reaction of the oxidation products from pure BCP ozonolysis with those formed in the presence of NO_2 and NO_3 radicals. In contrast, the mass spectra of non-N-containing organic species (org) at 213-243K showed no

substantial changes compared to the species from ozonolysis without nitrogen oxides present (cf. Fig.7). One obvious reason for this may be the lower NO₃ radical concentrations at lower temperatures but also changes in the active reaction pathways may play a role.”

L457-458: I am not sure if the “BCP ozonolysis in the presence of NO₃ radicals” is the right wording here. If I understand correctly, the BCP oxidation in the last stage of the experiment occurs in the presence of both oxidants.

We have modified this sentence as follows:

“Thus, it can be concluded that higher temperatures favour the formation of higher oxygenated organonitrates from the BCP oxidation in the presence of O₃, NO₂, and NO₃ radicals.”

Fig. S3 I struggle to differentiate the modelled from the measured ozone. Additionally, the reaction rates should have different units?

We have modified figure S5 (numbered as figure S3 before) to better distinguish between measured (symbols) and modelled data (lines). Reaction rates have units of cm³ molecule⁻¹ s⁻¹.

Please also re-check figure numbering.

We thank the reviewer for the kind reminder! We have checked the figure numbering.

References

Cox et al., (2020), Evaluated kinetic and photochemical data for atmospheric chemistry: Volume VII – Criegee intermediates. *Atmos. Chem. Phys.*, 20, 13497–13519, <https://doi.org/10.5194/acp-20-13497-2020>

Farmer et al., (2010), Response of an aerosol mass spectrometer to organonitrates and organosulfates and implications for atmospheric chemistry, *P. Natl. Acad. Sci. USA*, 107, 6670–6675, <https://doi.org/10.1073/pnas.0912340107>

Kundu et al., (2017), Molecular formula composition of β-caryophyllene ozonolysis SOA formed in humid and dry conditions, *Atmospheric Environment*, 154, 2017, 70-81, <https://doi.org/10.1016/j.atmosenv.2016.12.031>.

Lopez-Hilfiker et al., (2016), Constraining the sensitivity of iodide adduct chemical ionization mass spectrometry to multifunctional organic molecules using the collision limit and thermodynamic stability of iodide ion adducts, *Atmos. Meas. Tech.*, 9, 1505–1512, <https://doi.org/10.5194/amt-9-1505-2016>

Mellouki et al., (2021), Evaluated kinetic and photochemical data for atmospheric chemistry: volume VIII – gas-phase reactions of organic species with four, or more, carbon atoms (≥ C₄). *Atmos. Chem. Phys.*, 21, 4797–4808, <https://doi.org/10.5194/acp-21-4797-2021>

Reviewer #2

In the study by Gao et al., the authors explore the oxidation of β -caryophyllene (BCP) by dark ozonolysis performed in the AIDA atmospheric simulation chamber with and without the presence of nitrogen oxides at different temperatures. From state-of-the-art analytical techniques, the authors report on the formation and composition of resulting gas- and particle-phase secondary organic aerosol (SOA). Presented results show that temperature effects both SOA yields as well as chemical composition which the authors attribute to temperature-dependent difference in vapour pressure of the BCP oxidation products. Following initial ozonolysis of BCP, the influence of nitrogen oxides is examined by the addition of nitrogen dioxide and additional BCP to the ozone-filled chamber. In the presence of nitrogen oxides, the authors show formation of organonitrates contribution to the SOA with higher contributions of more oxygenated species observed at higher temperatures.

The manuscript provides new and important findings on the temperature-dependent formation of SOA from BCP. The applied analytical techniques are comprehensive including both gas and particle phase characterization of the formed SOA. The manuscript is well written, the results are clearly presented and discussed, and the topic falls within the scope of ACP. I thus recommend this work for publication once the following comments have been addressed.

General comments:

Discussions on the chemical compositions is mostly based on data from experiment 1a (213K) and 5a (313K). However, in experiment 1a knowledge of the experimental conditions are incomplete from the lack of BCP measurements. In general, the reviewer finds that all experiments vary in their execution and experimental conditions other than temperature. In particular, large variation in BCP concentrations, RH and BCP/Ozone ratios are noted. How do the authors justify comparison between experiments and in particular to exp. 1a?

Indeed, BCP was subject to rapid wall loss at 213K. However, in the presence of an excess of ozone, BCP was oxidized faster than the wall loss and we could generate a SOA mass load comparable to the other experiments. Due to similar BCP addition times, ozone levels, and SOA mass concentrations we consider it justified to use this experiment for comparison. Furthermore, we discuss the general trend of changes among all five temperatures studied and in this sense the experiment at 213 K is no outlier.

Could the author comments on the expected phase-state of the formed SOA particles under the studied conditions? With the large temperature and RH span, the authors should consider this for

two at least two reasons; 1) the partitioning of organics (e.g. semi-volatile org and org-Ns species) to the preexisting SOA particles (e.g. Bastelberger, 2017) and 2) particle-bound (surface or bulk) reactions (e.g. Shiraiwa, 2011). With respect to the latter, particle phase-state (solid or liquid) could affect both surface oxidation processes by ozone and OH-radicals but might also affect the proposed formation of dimers through esterification.

This question is addressed in our response to the general comment 2 of reviewer 1 and we have added the following text to the manuscript.

“Please note that we can’t exclude completely that the changing humidity in our experiments has no influence on our results. Nonetheless, we think that the SOA composition we have observed is dominated by gas phase reactions with sufficient water concentrations compared to ambient conditions and that the potential impact of relative humidity on condensed phase reactions was minimized by increasing relative humidity with decreasing temperature (Li and Shiraiwa, 2019; Maclean et al., 2021), maybe except for the lowermost temperature.”

The authors calculate OH-radical yield under the studied conditions and find significantly higher yields at elevated temperatures (5% at 243K vs 15% at 313K). However, due to the fast reaction of ozone with the endocyclic double bond of BCP 91-92% of BCP are calculated to react with ozone under the studied conditions, hence rendering contributions of OH-oxidation of BCP minor. However, considering that the authors attribute formation of higher oxidized compounds to further gas-phase oxidations of first-generation products, it would be worthwhile to discuss the influence of OH-radicals in this regard. In Witkowski (2019), several oxidation products from the OH + β -caryophyllonic acid has been identified including many found in the gas and particle phase of the current study, including C₄H₆O₄ and C₁₄H₂₂O₄, with the former identified in gas-phase SOA in 298K and 313K experiments only (Fig. 5).

Witkowski et al. (2019) identified and reported the main oxidation products from β -caryophyllonic acid (C₁₅H₂₄O₃) reacting with OH radicals in the aqueous phase. The main oxidation products they presented included C₁₄H₂₂O₄, C₁₅H₂₄O₅, C₁₅H₂₆O₆, C₁₅H₂₆O₅, C₁₄H₂₂O₆, C₉H₁₄O₄, C₄H₆O₄, and C₅H₈O₄. As we did not use any OH scavenger in our study, also oxidation products from gas phase reactions of OH radicals with products from BCP oxidation, like β -caryophyllonic acid, were observed. At higher temperatures, β -caryophyllonic acid is present in the gas phase and may partially be oxidized by the OH radicals formed in the first few minutes of the experiments by BCP ozonolysis. However, some of these products can also be formed via BCP reacting with ozone in the presence of OH scavengers (Li et al., 2011; Richters et al., 2016). Thus, C₄H₆O₄ can be an indicator of the OH radical related reactions in the gas phase, considering its low molecular weight and hence expected high vapor pressure. From Fig.5, the C₄H₆O₄ is more abundant at higher temperatures (298K, 313K), and it indicates the OH radical related reactions are more substantial which is consistent with our OH yield estimation (to be higher at enhanced temperatures).

On the composition of both gas and particle phase SOA data are presented as normalized signals to total gas or particle C_xH_yO_z(%), respectively, at the given temperature. Whilst this provides a clear picture of the changes to the chemical composition, it fails to report on the differences in concentration of individual species between experiments. For example, in Fig. 5, showing the average CIMS gas phase mass spectra, even at low 213K and 243K gas-phase species seems to be abundant. It would be beneficial to include (in the SI) the absolute signals of the identified

compounds, thus to be able to note the differences in abundance of these species between the experiments. As shown in Fig. 5, one might conclude that the gas-phase contain less organic compounds thus undermining the statement of gas-phase oxidation of first generation oxidation products as possible source to more oxidized monomers in particles formed at elevated temperatures. Also, as no BCP could be detected in the gas-phase at 213K due to wall-losses, how do the authors explain the detection of the oxidized species in Fig. 5?

We added the absolute signals of all detected gas phase compounds for all five temperatures in the supplement (Fig. S8). Figure R5 shows for the experiment at 213K almost no SOA formation after addition of ozone after the first addition of BCP. The initially added BCP went to the wall very fast and wasn't present for oxidation when ozone was added subsequently 30 min after the end of the first BCP addition. However, when we added BCP for a second time in the presence of ~300 ppb ozone in the chamber we observed substantial SOA formation as the BCP was oxidized before it was lost to the walls. We discuss the results from the experiment at 213K referring to the oxidation products from the ozonolysis of the second addition of BCP.

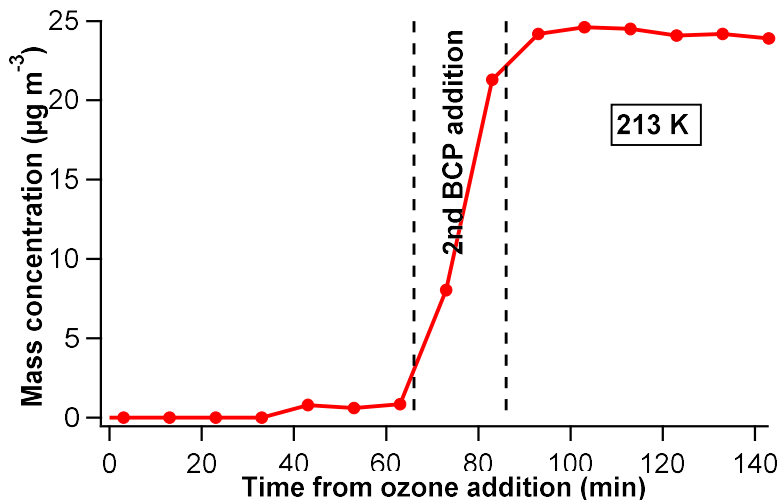


Figure R5. Time evolution of particle mass concentration measured by SMPS in the experiment at 213K.

We have added the following text to section 2.1:

“During the experiment at 213 K the initially added BCP was lost to the walls, so almost no SOA was formed after the addition of ozone. However, when adding BCP in the presence of ozone, SOA was formed in quantities comparable to the other experiments.”

Specific comments:

The general experimental protocol is unclear and seems to vary between experiments. From Fig.2 and table 1, two ozonolysis experiments without NO₂ (2a and 4a) include more than one addition of BCP. What is the reason for this?

During the experiments, we increased the SOA mass concentrations as to achieve comparable levels among the different experiments. We compared the particle chemical composition for these

two additions of BCP and found their mass spectra were similar (before/after the second BCP addition) for all experiments. We have explained this in section 2.1 as follows:

“After depletion of the BCP at a lower ozone level to facilitate the kinetic study we increased the excess of ozone to accelerate the oxidation of remaining double bonds. Yields and chemical compositions are determined and compared for the time period after increasing the ozone level.”

Fig 2 indicates that the initial oxidation of the added BCP ($65 \mu\text{g m}^{-3}$) was performed using a lower ozone concentration (25 ppb) than stated in table 1 (325 ppb). Please clarify.

The first ozone addition of ~ 25 ppb allowed studying the kinetics of the BCP + ozone reaction. After the BCP was consumed and the particle concentration became stable we increased the ozone concentration to ~ 300 ppb to accelerate the reaction of the second double bond of the BCP and to make the SOA comparable with others formed at other temperatures. Table 1 states the sum of both ozone additions. We have explained this in the method section as mentioned in the previous comment.

It is not apparent to the reviewer, whether results from yield calculations and chemical analysis relates to SOA formed after the initial (time 0, low ozone, Fig. 2) ozonolysis or following the second addition of BCP at much higher O_3 concentration (300 ppb).

The yields and chemical composition at all temperatures are related to the SOA at higher O_3 concentration (300 ppb), shown as the time period 50-80 min in Fig. 2. We have explained this in the method section as follows:

“Yields and chemical composition are determined and compared for the time period after increasing the ozone level.”

Despite the typical high time resolution and sensitivity of the PTR-ToF-MS no BCP measurements are reported during the two additions of BCP in Fig. 2. Why is this? If the rate by which BCP is added is the same during the two additions, it would have been useful to see how the loss of BCP changes under the studied conditions.

We have three additions of BCP in total in Fig. 2. The first BCP addition was done before time zero (addition of ozone) in Fig. 2, and its subsequent decay due to reaction with ozone was detected by PTR-TOF-MS. The second and third BCP addition were at ~ 76 -86 min and ~ 148 -160 min as indicated in Fig. 2. Due to the fast reaction of BCP with the excess of ozone the BCP concentrations did not reach a detectable level. However, as the BCP additions were done using the same device and conditions (e.g., temperature, flowrate), their addition rates can be expected to be very similar. However, the BCP losses were faster for the second and third BCP addition due to higher ozone levels compared to that for the initial BCP addition.

Line 126-128: the authors refer to the low vapour pressure and strong wall losses as possible explanation for the lacking BCP measurements at low temperatures. If all BCP is lost to the chamber walls, from where do the SOA particle mass form? Reactions on the chamber surfaces? if so, how can the authors account for this in their experiments?

At the lowest temperature (213K), we couldn't detect any BCP during its addition. We then added ~320 ppb of ozone (time zero) but only observed relatively weak SOA formation (~0.6 $\mu\text{g m}^{-3}$) after ~40 min, as shown in Figure R5, 66 minutes after ozone addition we added BCP again. The particle concentration increased quickly within several minutes due to the rapid reaction between BCP and ozone. Thus, we conclude that the BCP from the first addition was mainly lost to the wall and had only minor contributions to the SOA formed. Therefore, this experiment can be used for comparison with the other experiments just excluding the initial BCP addition. Potential reactions on the chamber surfaces have no impact on our results because potential reactants and reaction products typically stay adsorbed on the aluminum oxide surface of the wall. We have explained this also in the last General Comment by Reviewer 2 and added the following text to the manuscript:

“During the experiment at 213 K the initially added BCP was lost to the walls, so that almost no SOA was formed after the addition of ozone. However, when adding BCP in the presence of ozone, SOA was formed in quantities comparable to the other experiments.”

Line 147-148: Do the authors expect any issues from operating all instruments at 296K? This is significantly higher than experimental conditions of 213K and lower than 313K, thus may produce bias in the gas and particle phase measurements from evaporation and condensation of semi-volatile species during sampling.

This is indeed an important point. The temperature difference between the simulation chamber and the instruments is a general problem potentially causing biases e.g. due to phase partitioning of oxidation products. To minimize this, we enhanced the sampling flow rates of the instruments, i.e., FIGAERO-iodide-CIMS to shorten the residence times in the sampling tubes, and used thermal insulation materials to reduce the temperature change in the sampling lines, i.e., PTR-TOF-MS. In addition, Huang et al. (2018) has shown for α -pinene SOA for similar sampling procedures at the AIDA chamber that CIMS mass spectra were nearly identical for sampling at different temperatures.

We have explained this by adding the following sentence to the Method section 2.2:

“To avoid potential artifacts, e.g. due to phase partitioning of semi-volatile species in the sampling lines from the chamber to the instruments, the sampling lines were partially insulated and the residence time was below 1-2 seconds.”

Line 191-195: How many particle samples were collected for each experiment and how often were these collected? If multiple samples were collected, showing the evolution of the spectra or specific species (i.e. dimers and trimers) over time could be beneficial.

Particle samples were collected at the stages when the particle concentrations reached stable levels and thus have much lower time resolution than the gas phase data. The red triangles in the middle panel of Fig. 2 show mass concentrations of the particle samples analyzed by FIGAERO-CIMS. The mass spectra, mass loadings, and the signal fractions of specific species were similar for the two particle samples which were collected at the same stage, e.g., for 213K. Thus, the mass spectra shown in the manuscript is the average of the two samples collected at the same stage. We have added the information on the amount of particle samples to section 2.2 as follows:

“We collected 4, 3, 3, 2, 2 particle filter samples for the periods when the particle concentrations reached stable levels in experiments at 213 K, 243 K, 273K, 298K, and 313 K, respectively.”

Line 240-241: it would be useful if the authors provided similar figures as Fig. 2 (in SI) for all experiments conducted. Also, the authors should state the maximum particle number concentration and particle size (Table 1 og SI).

The time evolution of all other experiments (213K, 243K, 273K, and 313K) are added in the supplement as Figure S4, including the mass concentration and particle number concentration distribution over all the periods. The particle sizes which contribute most to the mass concentration are also added to Table 1 in the manuscript.

Line 251: Did the authors observe new particle formation following the last injection of BCP in all experiments?

As shown in Figures 2 and S4 (supplement), small particles with diameters of 20-40 nm were formed after the last injection of BCP at 298K and 313K. However, at 213-273K, no new particle formation was observed for particles larger of 13 nm following the last addition of BCP.

Line 278-279: What was the reasoning behind not applying OH-scavengers and seed particles to the experiments?

We did not use OH-scavengers in the experiments because we wanted to study not only the products from ozonolysis but also from OH radical reactions. However, due to the high reactivity of BCP towards ozone, the relative high ozone concentrations, and the relatively low OH radical yields from BCP ozonolysis, we can expect the product distribution being dominated by the ozonolysis reaction. The reason for not using seed particles is that the volatilities of the oxidation products from β -caryophyllene are expected to be low enough to form new particles even without additional pre-existing particle surfaces.

Line 354-355: How do the concentration/relative signal of dimers and monomer change over time? If dimers are formed from esterification of monomers, this could be evident from continuous increase of dimeric compounds after BCP depletion. In SI only time resolved data of monomeric species are shown.

Dimers were found abundantly at 213-243K in the particle phase. However, the gas phase signal of individual dimeric molecules at 213-243K was almost zero and showed no significant change over the experiments, potentially due to the extremely low volatilities at such cold temperatures for those large molecular-weight species with 28-30 carbon atoms and 5-9 oxygen atoms. We found a slight increase of gas phase signals after the 2nd BCP addition only by summing up all signals of dimers (Figure R6). This may also be an indicator for the dimer formation via esterification from monomers.

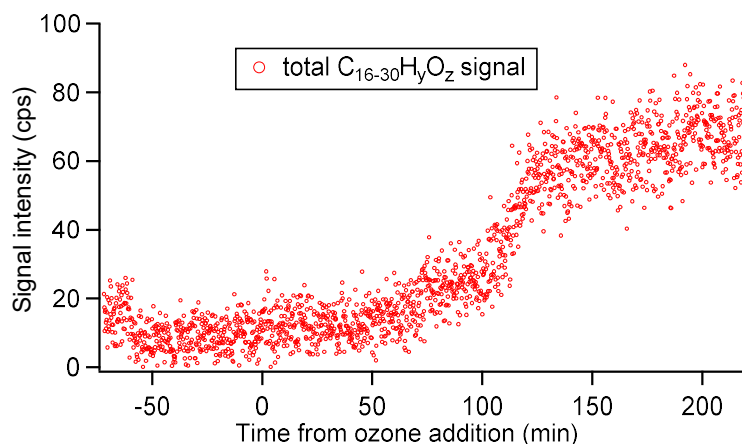


Figure R6. Time evolution of the signal intensity of the sum of all $C_{16-30}H_yO_z$ species.

Line 356-358: Why are the dimeric molecules not observed at temperatures above 273K, despite the presence of the monomeric precursors?

The dimers which were formed at temperatures above 273K were more oxygenated than the dimers formed at 213-243K (cf. Fig. 6), and thus, these two types of dimers should have different monomer precursors. At 213-243K, the dimers are dominated by the lower oxygenated species (DLOC, $C_{28-30}H_yO_{5-8}$), with potential precursors of first-generation oxidation monomeric products, e.g., $C_{15}H_{24}O_3$. However, with the temperature increasing, the β -caryophyllene is oxidized more via the autoxidation pathways, preventing the formation such compounds. Hence, less DLOC dimers were formed. At temperatures above 273K, highly oxygenated monomers, which are expected to have low volatilities, form higher oxygenated dimers (DHOC, $C_{28-30}H_yO_{9-11}$). Between 243-273K there seems to be the tuning point between these two mechanisms and may explain that we find the lowest dimer fraction at 273K (cf. Fig. 8).

Technical corrections

Line 354: Remove punctuation mark after "...vapor pressure"

This was removed.

References

Witkowski B, Al-sharafi M, Gierczak T (2019) Kinetics and products of the aqueous-phase oxidation of β -caryophyllonic acid by hydroxyl radicals, *Atmospheric Environment*, 213, 231-238,

Bastelberger S, Krieger UK, Luo B, & Thomas P (2017) Diffusivity measurements of volatile organics in levitated viscous aerosol particles. *Atmospheric Chemistry and Physics* 17(13):8453-8471

Shiraiwa M, Ammann M, Koop T, & Pöschl U (2011) Gas uptake and chemical aging of semisolid organic aerosol particles. *Proceedings of the National Academy of Sciences* 108(27):11003-11008.

Reference for Response

Kundu, S., Fisseha, R., Putman, A. L., Rahn, T. A., and Mazzoleni, L. R.: Molecular formula composition of β -caryophyllene ozonolysis SOA formed in humid and dry conditions, *Atmospheric Environment*, 154, 70-81, <https://doi.org/10.1016/j.atmosenv.2016.12.031>, 2017.

Li, Y., and Shiraiwa, M.: Timescales of secondary organic aerosols to reach equilibrium at various temperatures and relative humidities, *Atmos. Chem. Phys.*, 19, 5959-5971, 10.5194/acp-19-5959-2019, 2019.

Li, Y. J., Chen, Q., Guzman, M. I., Chan, C. K., and Martin, S. T.: Second-generation products contribute substantially to the particle-phase organic material produced by β -caryophyllene ozonolysis, *Atmos. Chem. Phys.*, 11, 121-132, 10.5194/acp-11-121-2011, 2011.

Macleán, A. M., Smith, N. R., Li, Y., Huang, Y., Hettiyadura, A. P. S., Crescenzo, G. V., Shiraiwa, M., Laskin, A., Nizkorodov, S. A., and Bertram, A. K.: Humidity-Dependent Viscosity of Secondary Organic Aerosol from Ozonolysis of β -Caryophyllene: Measurements, Predictions, and Implications, *ACS Earth and Space Chemistry*, 5, 305-318, 10.1021/acsearthspacechem.0c00296, 2021.

Richters, S., Herrmann, H., and Berndt, T.: Different pathways of the formation of highly oxidized multifunctional organic compounds (HOMs) from the gas-phase ozonolysis of β -caryophyllene, *Atmos. Chem. Phys.*, 16, 9831-9845, 10.5194/acp-16-9831-2016, 2016.

Donahue, N. M., Henry, K. M., Mentel, T. F., Kiendler-Scharr, A., Spindler, C., Bohn, B., Brauers, T., Dorn, H. P., Fuchs, H., Tillmann, R., Wahner, A., Saathoff, H., Naumann, K.-H., Möhler, O., Leisner, T., Müller, L., Reinnig, M.-C., Hoffmann, T., Salo, K., Hallquist, M., Frosch, M., Bilde, M., Tritscher, T., Barmet, P., Praplan, A. P., DeCarlo, P. F., Dommen, J., Prévôt, A. S. H., and Baltensperger, U.: Aging of biogenic secondary organic aerosol via gas-phase OH radical reactions, *Proceedings of the National Academy of Sciences*, 109, 13503-13508, 10.1073/pnas.1115186109, 2012.

Francisco, M. A., and Krylowksi, J.: Chemistry of Organic Nitrates: Thermal Chemistry of Linear and Branched Organic Nitrates, *Industrial & Engineering Chemistry Research*, 44, 5439-5446, 10.1021/ie049380d, 2005.

Lee, B. H., Mohr, C., Lopez-Hilfiker, F. D., Lutz, A., Hallquist, M., Lee, L., Romer, P., Cohen, R. C., Iyer, S., Kurtén, T., Hu, W., Day, D. A., Campuzano-Jost, P., Jimenez, J. L., Xu, L., Ng, N. L., Guo, H., Weber, R. J., Wild, R. J., Brown, S. S., Koss, A., Gouw, J. d., Olson, K., Goldstein, A. H., Seco, R., Kim, S., McAvey, K., Shepson, P. B., Starn, T., Baumann, K., Edgerton, E. S., Liu, J., Shilling, J. E., Miller, D. O., Brune, W., Schobesberger, S., D'Ambro, E. L., and Thornton, J. A.: Highly functionalized organic nitrates in the southeast United States: Contribution to secondary organic aerosol and reactive nitrogen budgets, *Proceedings of the National Academy of Sciences*, 113, 1516-1521, doi:10.1073/pnas.1508108113, 2016.

Li, Y., and Shiraiwa, M.: Timescales of secondary organic aerosols to reach equilibrium at various temperatures and relative humidities, *Atmos. Chem. Phys.*, 19, 5959-5971, 10.5194/acp-19-5959-2019, 2019.

Li, Y. J., Chen, Q., Guzman, M. I., Chan, C. K., and Martin, S. T.: Second-generation products contribute substantially to the particle-phase organic material produced by β -caryophyllene ozonolysis, *Atmos. Chem. Phys.*, 11, 121-132, 10.5194/acp-11-121-2011, 2011.

Macleán, A. M., Smith, N. R., Li, Y., Huang, Y., Hettiyadura, A. P. S., Crescenzo, G. V., Shiraiwa, M., Laskin, A., Nizkorodov, S. A., and Bertram, A. K.: Humidity-Dependent Viscosity of Secondary Organic Aerosol from Ozonolysis of β -Caryophyllene: Measurements, Predictions, and Implications, *ACS Earth and Space Chemistry*, 5, 305-318, 10.1021/acsearthspacechem.0c00296, 2021.

Naumann, K.-H.: COSIMA—a computer program simulating the dynamics of fractal aerosols, *Journal of Aerosol Science*, 34, 1371-1397, [https://doi.org/10.1016/S0021-8502\(03\)00367-7](https://doi.org/10.1016/S0021-8502(03)00367-7), 2003.

Richters, S., Herrmann, H., and Berndt, T.: Different pathways of the formation of highly oxidized multifunctional organic compounds (HOMs) from the gas-phase ozonolysis of β -caryophyllene, *Atmos. Chem. Phys.*, 16, 9831-9845, [10.5194/acp-16-9831-2016](https://doi.org/10.5194/acp-16-9831-2016), 2016.

Saathoff, H., Naumann, K., Möhler, O., Jonsson, A., Hallquist, M., Kiendler-Scharr, A., Mentel, T. F., Tillmann, R., and Schurath, U.: Temperature dependence of yields of secondary organic aerosols from the ozonolysis of α -pinene and limonene, *Atmos. Chem. Phys.*, 9, 1551-1577, 2009.